2015-04

Channelling of hydrothermal fluids during the accretion and evolution of the upper oceanic crust: Sr isotope evidence from ODP Hole 1256D

Harris, M

http://hdl.handle.net/10026.1/3524

Channelling of hydrothermal fluids during the accretion and evolution of the upper oceanic crust: Sr isotope evidence from ODP Hole 1256D

CrossMark

Michelle Harris *, Rosalind M. Coggon, Christopher E. Smith-Duque, Matthew J. Cooper, James A. Milton, Damon A.H. Teagle

Ocean and Earth Science, National Oceanography Centre Southampton, University of Southampton, European Way, Southampton, SO14 3ZH, UK

A B S T R A C T

ODP Hole 1256D in the eastern equatorial Pacific is the first penetration of a complete section of fast spread ocean crust down to the dike–gabbro transition, and only the second borehole to sample in situ sheeted dikes after DSDP Hole 504B. Here a high spatial resolution record of whole rock and mineral strontium isotopic compositions from Site 1256 is combined with core observations and downhole wireline geophysical measurements to determine the extent of basalt–hydrothermal fluid reaction and to identify fluid pathways at different levels in the upper ocean crust.

The volcanic sequence at Site 1256 is dominated by sheet and massive lava flows but the Sr isotope profile shows only limited exchange with seawater. However, the upper margins of two anomalously thick (>25 m) massive flow sequences are strongly hydrothermally altered with elevated Sr isotope ratios and appear to be conduits for lateral low-temperature off-axis fluid flow. Elsewhere in the lavas, high $^{87}Sr/^{86}Sr$ are restricted to breccia horizons. Mineralised hyaloclastic breccias in the Lava–Dike Transition are strongly altered to Mg-saponite, silica and pyrite, indicating alteration by mixed seawater and cooled hydrothermal fluids. In the Sheeted Dike Complex $^{87}Sr/^{86}Sr$ ratios are pervasively shifted towards hydrothermal fluid values (~0.705). Dike chilled margins display secondary mineral assemblages formed during both axial recharge and discharge and have higher $^{87}Sr/^{86}Sr$ than dike cores, indicating preferential fluid flow along dike margins. Localised increases in $^{87}Sr/^{86}Sr$ in the Dike–Gabbro Transition indicates the channelling of fluids along the sub-horizontal intrusive boundaries of the 25 to 50 m-thick gabbroic intrusions, with only minor increases in $^{87}Sr/^{86}Sr$ within the cores of the gabbro bodies.

When compared to the pillow lava-dominated section from Hole 504B, the Sr isotope measurements from Site 1256 suggest that the extent of hydrothermal circulation in the upper ocean crust may be strongly dependent on the eruption style. Sheet and massive flow dominated lava sequences typical of fast spreading ridges may experience relatively restricted circulation, but there may be much more widespread circulation through pillow lava-dominated sections. In addition, the Hole 1256D sheeted dikes display a much greater extent of Sr-isotopic exchange compared to dikes from Hole 504B. Because seawater-derived hydrothermal fluids must transit the dikes during their evolution to black smoker-type fluids, the different Sr-isotope profiles for Holes 504B and 1256D suggest there are significant variations in mid-ocean ridge hydrothermal systems at fast and intermediate spreading ridges, which may impact geochemical cycles of elements mobilised by fluid–rock exchange at different temperatures.

1. Introduction

Seawater circulation through, and reaction with, the ocean crust is a fundamental Earth process that controls the magmatic accretion of new oceanic crust, modifies the composition of ocean crust and seawater, and through subduction transports surficial geochemical signatures to the mantle. At mid ocean ridges (MOR) hydrothermal circulation is most spectacularly expressed as high temperature (up to 400 °C) vent fluids, but at the ridge axis and ridge flanks, lower temperature (<150 °C) hydrothermal circulation is also important. Because vent fluids provide only limited information on the subsurface, we require improved knowledge on sub-surface fluid flow pathways, and the vigour and longevity of seafloor hydrothermal alteration to further understand magmatic accretion at MOR (e.g., Henstock et al., 1993; Kelemen et al., 1997)

* Corresponding author. Tel.: +44-2380-596539.
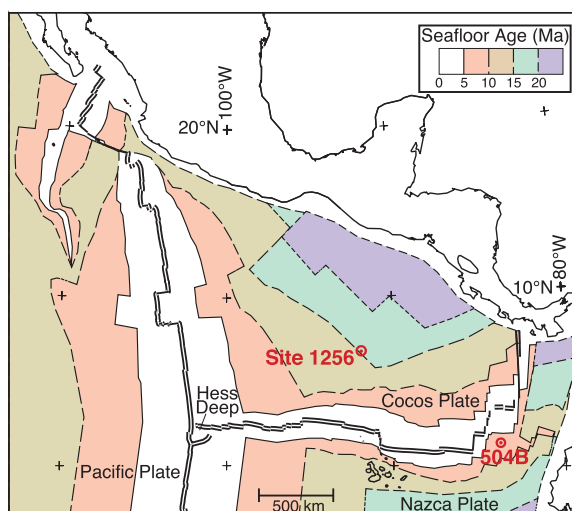*E-mail address:* michelle.harris@noc.soton.ac.uk (M. Harris).

Fig. 1. Map of the locations of Site 1256 and Site 504 with crustal age shown in 5 million year intervals (modified from Wilson et al., 2003).

and better quantify the influence of seawater-basalt exchange on global chemical cycles (e.g., Vance et al., 2009).

To date, much of our knowledge of MOR hydrothermal circulation is reflected by conceptual cartoons developed from active and passive seismic observations (e.g., Kent et al., 1990; Tolstoy et al., 2008), measurements of vent fluid chemistry, thermal models, and core descriptions from ocean crust "reference site" DSDP Hole 504B (Alt, 1995). Unfortunately, observations from ophiolites appear inappropriate for MOR hydrothermal systems (e.g., Alt and Teagle, 2000; Bickle and Teagle, 1992), so key questions remain unresolved principally due to a dearth of direct information from intact ocean crust. For example, many sketches of MOR hydrothermal circulation indicate focused lateral fluid movement along the top of axial magma chambers, but to date there is only limited evidence for such flow. Sheeted sill-type models of ocean crust accretion require deep hydrothermal fluid circulation to remove latent and sensible heat from the lower crust (Maclennan et al., 2004) but the conduits for the downwelling of cool seawater-derived fluid remain elusive. Borehole observations and sampling by scientific ocean drilling is essential to better understand ocean floor hydrothermal systems but the paucity of deep holes into ocean crust limits our knowledge of seafloor basalt-hydrothermal alteration.

Here we present a high spatial resolution whole rock and mineral Sr isotope profile for ODP Site 1256, the first borehole to sample a complete section down to gabbros of intact upper ocean crust formed at a fast spreading rate (Teagle et al., 2006; Wilson et al., 2006). Our interpretations from this profile are tightly integrated with detailed petrography and geochemistry of the drill cores (Alt et al., 2010; Teagle et al., 2006; Wilson et al., 2003) and borehole wireline observations (Tominaga et al., 2009; Tominaga and Umino, 2010). We document sub-horizontal and sub-vertical channelling of seawater-derived hydrothermal fluids at different levels in the ocean crust, and develop a temporal model for the evolving hydrothermal system at Site 1256.

2. ODP Site 1256

ODP Site 1256 is situated in the Guatemala Basin on 15 million year-old ocean crust that formed at the East Pacific Rise (EPR) during an episode of superfast spreading (220 mm/yr, full rate; Fig. 1; Wilson, 1996). This location was selected for deep drilling to reach cumulate gabbros with the minimal depth pen-

etration by testing the inverse relationship between spreading rate and the depths to the axial low velocity zones imaged by multi-channel seismic experiments at MOR (Carbotte et al., 1998; Purdy et al., 1992). Hole 1256D has been deepened down to the dike–gabbro transition during 4 scientific drilling expeditions (ODP Leg 206, IODP Expeditions 309/312, 335) (Teagle et al., 2006, 2012a; Wilson et al., 2003, 2006).

Hole 1256D is only the second borehole to sample sheeted dikes in intact ocean crust following Hole 504B (Alt et al., 1993). Throughout the lavas and dikes, core recovery rates are higher in Hole 1256D than Hole 504B (Hole 1256D 41% and 37%, Hole 504B 30% and 14%, lavas and dikes respectively). Importantly, wireline geophysical logging was undertaken during each stage of the Hole 1256D drilling, and provides an unrivalled suite of continuous physical properties logs and borehole images (Tominaga et al., 2009). These data enable the partial characterisation of material not recovered during coring, the identification of axial and off-axis lava deposition, and the establishment of the sequence of volcanic eruption at Site 1256 (Tominaga et al., 2009; Tominaga and Umino, 2010).

2.1. Lithostratigraphy

The 1271.6 m of drilled basement at Site 1256 is overlain by 250 m of sediments (Wilson et al., 2003) (Fig. 2). The pilot basement Hole 1256C recovered the top 88 m of the volcanic crust not recovered in Hole 1256D because of the installation of casing. The volcanic sequence (250–1004.1 m below seafloor (mbsf)) includes lava flows erupted both on and off axis. The interpretation of off-axis deposition for the uppermost lavas is based on the requirement for significant topography to pond very thick lava flows (Lava Pond) and for the Inflated Flows to have been erupted onto a sub-horizontal surface. On-axis volcanism in Hole 1256D is characterised by sheet flows tens of centimetres to 3 m thick, and massive flows 3 m to 26 m thick. The Lava–Dike Transition (LDT) comprises a 55 m-thick interval of sheet and massive flows punctuated by discrete zones of breccia and mineralisation. The Sheeted Dike Complex (SDC) comprises aphyric basalt with subvertical intrusive contacts, with an average dike width of 0.5 m (Tominaga et al., 2009). The lowermost dikes were contact metamorphosed to granoblastic textures and granulite assemblages. The Dike–Gabbro Transition (DGT) is composed of two intrusive gabbro bodies (Gabbro 1, 52.3 m-thick and Gabbro 2, 24.0 m), separated by two granoblastically recrystallised dike screens (Dike Screen 1, 24 m and Dike Screen 2, 23 m). Dike Screen 2 hosts a post-contact metamorphism greenschist facies dike that preserves its igneous texture.

The thickness (>150 m) of strongly recrystallised granoblastic dikes requires greater thermal energy than is available from the two gabbro intrusions (Coggon et al., 2008; Koepke et al., 2008). This requires either a large magma chamber below the bottom of the hole or significant topography on the dike–gabbro boundary at Site 1256. The common occurrence in Dike Screen 2 of cm-scale felsic and gabbroic intrusions suggests that the region of ∼100% plutonic rocks is perhaps within a few tens of metres of the current base of the hole (Teagle et al., 2012a).

The core-based lithostratigraphy is complemented by a wireline logging-based volcanostratigraphy developed from continuous downhole geophysical properties to define 8 electrofacies and quantify their abundance and downhole distribution (Tominaga et al., 2009). Wireline data show that much of the volcanic sequence is dominated by fractured or fragmented flows (∼40%) and that breccias and dike margins are under-represented in the cores recovered.
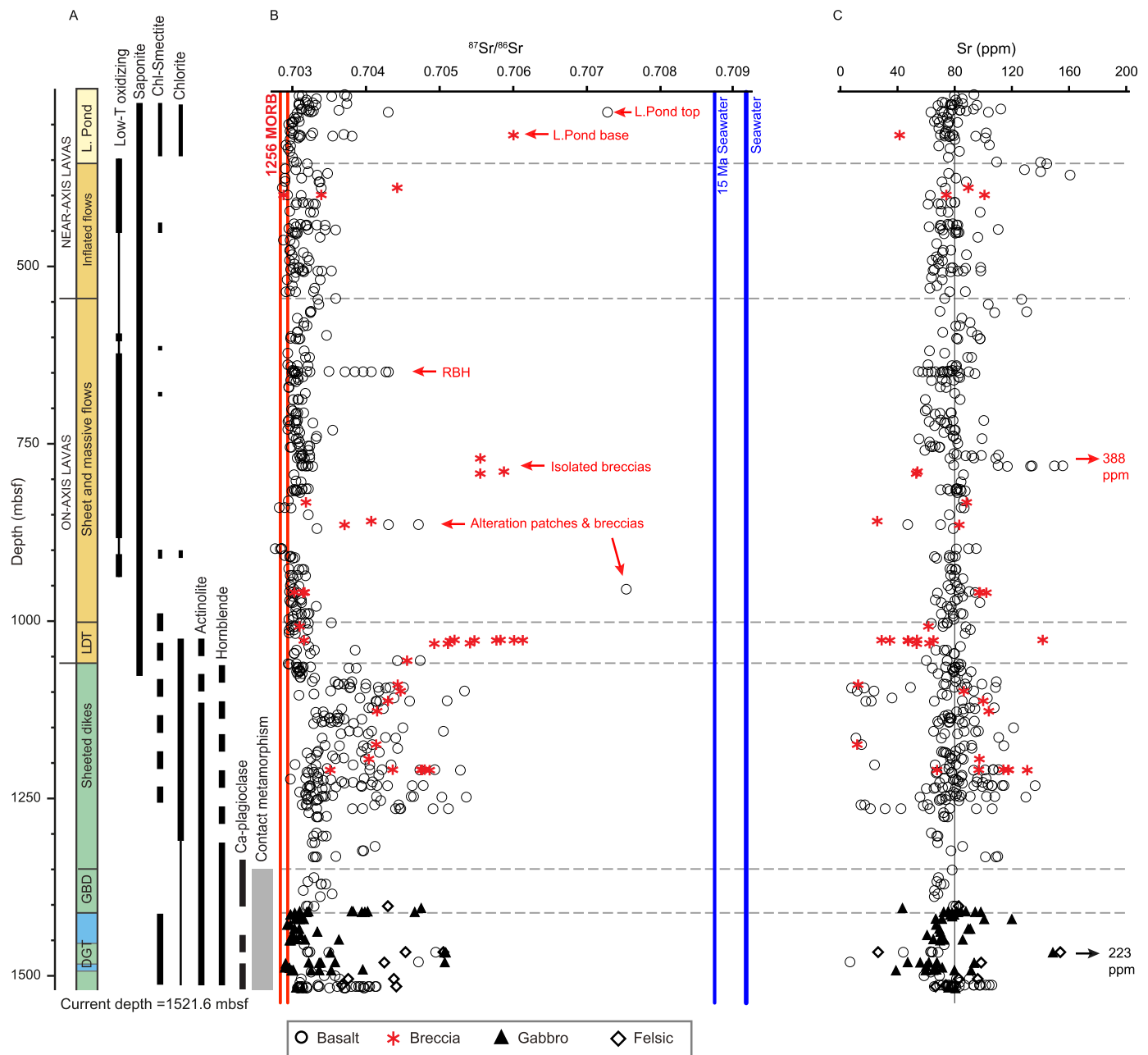
Fig. 2. (A) Downhole lithostratigraphy for Hole 1256D and secondary mineral occurrence from thin section observations (modified from Teagle et al., 2012a and Alt et al., 2010). (B) Whole rock $^{87}Sr/^{86}Sr$ isotope profile, shown relative to fresh Site 1256 MORB, 15 Ma seawater and modern day seawater. Whole rock samples are distinguished by rock type and are age corrected to 15 Ma (Supplementary Data B and Höfig et al., 2014). (C) Whole rock Sr concentrations for each rock type in Hole 1256D (Supplementary Data B).

2.2. Hydrothermal alteration

Hydrothermal alteration in the volcanic section is dominated by the formation of celadonite, iron oxyhydroxides, saponite, pyrite and late-stage carbonates and zeolites (earliest to latest) (Alt et al., 2010). Alteration is most strongly developed in vein halos, vein networks, breccias, and patches. The volcanic section does not display a simple downhole progression from relatively oxidised to reduced alteration assemblages and is characterised by a low abundance of oxyhydroxide alteration halos compared to other upper crustal locations (cf. Hole 504B, Alt, 2004). Temperatures of hydrothermal mineral formation, based on oxygen isotope measurements, increase with depth in the lavas from 50–135 °C, similar to upper crustal alteration observed elsewhere (Alt et al., 2010). In the Lava–Dike Transition there is a pronounced change with

depth from rocks altered at low temperatures to partial alteration to greenschist facies minerals such as actinolite, chlorite and albite.

In the Sheeted Dike Complex the earliest stage of hydrothermal circulation at 400–800 °C is recorded by the formation of secondary clinopyroxene, amphibole, chlorite, plagioclase, epidote, titanite and pyrite disseminated in the rocks and in veins, and whole rock base metal depletions (Alt et al., 2010). The lower dikes were subsequently contact metamorphosed to granoblastic textures by the intrusion of a large plutonic body (Alt et al., 2010; Coggon et al., 2008; Koepke et al., 2008; Teagle et al., 2006). The DGT records multiple alteration stages from early amphibolite to later greenschist assemblages (Alt et al., 2010). As the hydrothermal system waned, prehnite and laumontite formed in the dikes and gabbros. Whole rock $\delta^{18}O$ data is consistent with the observed

Table 1

Summary table of whole rock $^{87}Sr/^{86}Sr$ isotopes and Sr concentrations for each lithological unit in Site 1256D. Sr isotopes are age corrected to 15 Ma. The average $^{87}Sr/^{86}Sr$ for Hole 1256D is a weighted average based on the average $^{87}Sr/^{86}Sr$ for each unit and their relative thicknesses.

Stratigraphic unit	n	Recovery (%)	$^{87}Sr/^{86}Sr$ (t = 15 Ma)				Sr (ppm)	
			Minimum	Maximum	Average	1σ	Average	1σ
Fresh 1256 MORB	6	–	0.702834	0.702928	0.70287	0.00004	–	–
Lava pond	56	93.3	0.702912	0.707283	0.70333	0.00071	81	13
Inflated Flows	71	39.7	0.702879	0.704424	0.70320	0.00022	83	21
Sheet and Massive Flows	170	33.9	0.702835	0.707538	0.70322	0.00054	83	29
Lava–Dike Transition	23	26.9	0.703019	0.706131	0.70411	0.00114	69	23
Sheeted Dike Complex	187	37.1	0.702941	0.705363	0.70378	0.00056	79	24
Granoblastic dikes	9	6.5	0.703147	0.703539	0.70332	0.00013	71	6
Gabbro 1	29	30.6	0.702961	0.704750	0.70340	0.00053	79	14
Dike Screen 1	10	12.0	0.703158	0.705085	0.70410	0.00090	93	62
Gabbro 2	17	53.3	0.702899	0.705071	0.70351	0.00064	81	25
Dike Screen 2	42	4.4	0.703050	0.704411	0.70353	0.00041	82	11
All Hole 1256D	614	37.1	0.702835	0.707538	0.70343	0.00037	80	24

downhole trend in Hole 1256D of low to high temperature hydrothermal alteration (Gao et al., 2012).

3. Results

3.1. Sr isotope profile

The Sr isotope sampling was guided by petrographic descriptions (e.g., Alt et al., 2010; Teagle et al., 2006; Wilson et al., 2003) that provide a petrogenic framework to investigate evolving hydrothermal conditions (Supplementary Material A). In contrast to previous studies (e.g., Gao et al., 2012), whole rock samples have been subdivided into component parts that record different styles of hydrothermal interaction, such as breccias, vein halos, dike margins or patches, and analysed separately (Table 1 and Supplementary Material B). These analyses are complemented by Sr-isotopic measurements of secondary mineral from veins, breccia cements and patch fillings that record the $^{87}Sr/^{86}Sr$ of the fluids from which they precipitated (Supplementary Material C). All data have been age corrected to 15 Ma but the low Rb/Sr ratios of most samples results in only a minor adjustment in $^{87}Sr/^{86}Sr$.

The whole rock $^{87}Sr/^{86}Sr$ profile for Hole 1256 is constrained by fresh Site 1256 MORB, seawater (modern and 15 Ma, McArthur et al., 2001) and the estimated hydrothermal vent fluid composition. Fresh Site 1256 MORB was determined by multi-step leaching of weakly altered basalts ($^{87}Sr/^{86}Sr = 0.70283–0.70293$, n = 6) (Supplementary Material A). The end member high temperature hydrothermal vent fluid discharging at Site 1256 is based on epidote mineral separates from hydrothermal veins and alteration patches ($^{87}Sr/^{86}Sr$ 070505–0.70525, n = 5) (Supplementary Material B). Epidote is a common mineral in the sub-seafloor zones of black smoker systems and has high Sr concentrations so is less susceptible to low temperature overprinting. The Hole 1256D epidotes have higher $^{87}Sr/^{86}Sr$ than modern vent fluids from the EPR, but are consistent with the trend between spreading rate and $^{87}Sr/^{86}Sr$ of modern vent fluids extrapolated to superfast spreading rates (Bach and Humphris, 1999).

Most whole rock samples have $^{87}Sr/^{86}Sr$ that are elevated from fresh MORB (Fig. 2B; Table 1, Supplementary Material B). The mean $^{87}Sr/^{86}Sr$ for all whole rock samples is 0.70349 (1σ = 0.00063, n = 614), and a weighted mean calculated using the mean $^{87}Sr/^{86}Sr$ for each stratigraphic unit and the relative proportion of each unit in the Hole is 0.70343 (1σ_w = 0.00037, n = 614). The weighted mean using the electrofacies classification of the Hole 1256D volcanic sequences (Tominaga et al., 2009), assuming that recovered cores for each electrofacies are representative, is 0.70344 ± 0.01960 (n = 483). However, as fragmented material is likely to be more altered, the $^{87}Sr/^{86}Sr$ of the recovered cores are likely biased to

lower values. If the unrecovered material is instead more similar to the highest $^{87}Sr/^{86}Sr$ for those electrofacies, the weighted average for Hole 1256D is ∼0.7038.

The $^{87}Sr/^{86}Sr$ profile in the volcanic sequence shows no overall trend with depth and there is no discernible difference between flow types or lavas emplaced on or off axis (Fig. 3). Seventeen highly altered whole rock samples from breccia horizons throughout the volcanic section and the extensively altered "Red Brick Horizon" (RBH) (650 mbsf) punctuate the $^{87}Sr/^{86}Sr$ profile with elevated ratios. Low temperature secondary minerals precipitated in veins (saponite, celadonite, chlorite, carbonate) generally record decreasing $^{87}Sr/^{86}Sr$ compositions with depth (Supplementary Material C, Coggon et al., 2010). Mineralised breccia horizons in the Lava–Dike Transition have higher $^{87}Sr/^{86}Sr$ than the surrounding sheet flows.

Rocks from the Sheeted Dike Complex have a wide range of $^{87}Sr/^{86}Sr$ in the upper 210 m of the SDC, whereas the Granoblastic Dikes although still elevated, show a more limited range in $^{87}Sr/^{86}Sr$. Chilled, brecciated and mineralised dike margins, along with narrow intrusive dikelets, exhibit significantly higher $^{87}Sr/^{86}Sr$ values than the background dikes.

The two gabbro bodies have elevated $^{87}Sr/^{86}Sr$ along their boundaries, but only minor increases in the centres of the bodies. In both intrusions $^{87}Sr/^{86}Sr$ is more strongly shifted along the upper boundary. Amphibole vein Sr-isotope compositions are more rock-like than the epidote hydrothermal fluid end member (Supplementary Material B). Both Dike Screen 1 and Dike Screen 2 display a wide range of $^{87}Sr/^{86}Sr$, with samples containing felsic intrusions recording the highest $^{87}Sr/^{86}Sr$. Alteration halos that overprint the granoblastic recrystallisation have higher $^{87}Sr/^{86}Sr$ than the adjacent background recrystallised basalts, indicating continuing hydrothermal exchange subsequent to the contact metamorphism.

3.2. Sr mobility

Sr is generally insensitive to magmatic fractionation, this prevents definition of a clear magmatic trend for the least altered samples to compare to the more altered samples (Coogan and Dosso, 2012). In the absence of a quantitative method for estimating the initial Sr concentration, the simplest approach for assessing Sr mobility with the least assumptions is to observe the downhole variation in Sr concentration (Fig. 2). The total variation in Sr concentration in Hole 1256D is 7–338 ppm (mean Sr = 80 ppm, 1σ = 25 ppm, Table 1), but ∼90% of all background alteration samples lie within 60–100 ppm, that likely reflects primary igneous concentrations. Hence, fluid–rock interaction in Hole 1256D generally involves isotopic exchange with only minor changes in
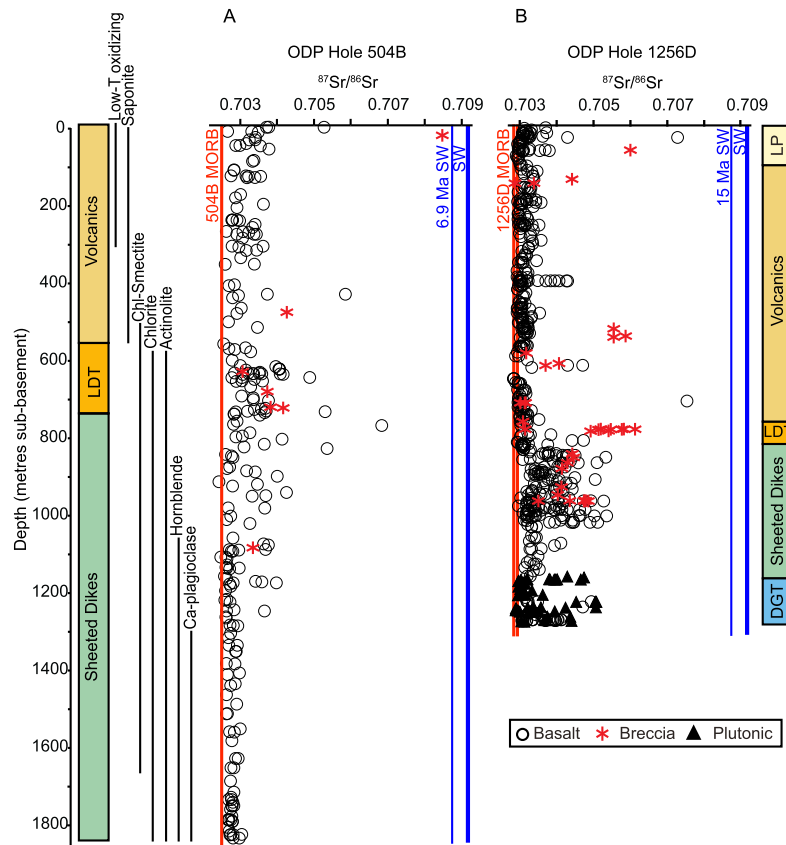
Fig. 3. Lithostratigraphy and Sr isotope profiles for Holes 504B and Hole 1256D demonstrate the variability in whole rock Sr isotope exchange between the two deep drill holes into intact ocean crust. Samples are plotted as metres sub-basement to account for different sediment thickness. Whole rock data are age corrected to 6.9 Ma (Hole 504B) and 15 Ma (Hole 1256D). Hole 504B whole rock data compiled from Bach et al. (2003), Teagle et al. (1998a, 1998b) and Teagle (unpublished).

Sr content through mineral precipitation. The more altered samples (breccias, alteration halos and patches) have a wider range of Sr concentrations matching the secondary minerals present. In samples with low Sr concentrations, igneous phases have been replaced or diluted by Sr-poor secondary minerals such as quartz and sulphides. Similarly, the highest Sr concentrations are associated with high-Sr secondary minerals such as epidote.

4. Discussion

4.1. Comparison with DSDP Hole 504B

Hole 504B is located 200 km south of the Costa Rica Rift (Fig. 1) and penetrates 1836 m into 6.9 Ma crust that formed at an intermediate spreading rate. Hole 504B samples 571.5 m of volcanic rocks, a 209 m-thick Lava–Dike Transition and 1056 m of Sheeted Dike Complex (Fig. 3) (Alt et al., 1993). Pillow lavas are most common in Hole 504B, in contrast to the sheet and massive flows abundant in Hole 1256D. Also, the Lava–Dike Transition and Sheeted Dike Complex in Hole 504B are substantially thicker. Although the same secondary minerals are present in the volcanic sequences of both holes, there is a much greater abundance of oxidation halos in the uppermost portions of the Hole 504B crust (Alt, 2004; Alt et al., 1996a, 1996b; Wilson et al., 2003). The sequence of secondary mineral occurrence with depth in both the sheeted dike complexes is similar, but the different thickness of the dike layers must reflect drastically different thermal gradients in this zone between the lavas and the underlying magma chambers (Teagle et al., 2006).

The differences between Holes 1256D and 504B are pronounced in their Sr isotope profiles (Fig. 3) (Bach et al., 2003; Teagle et al.,
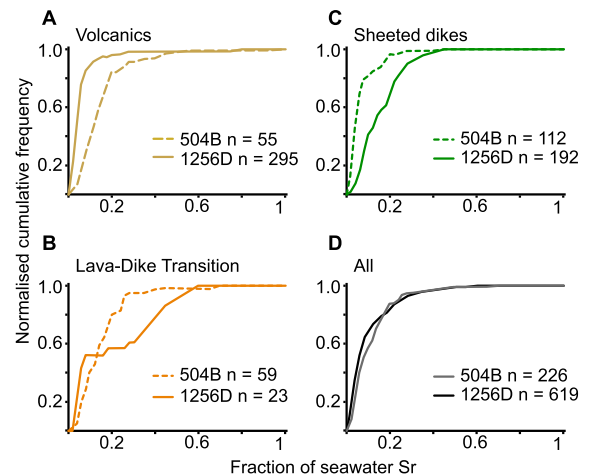

Fig. 4. Normalised cumulative frequency diagrams for each major stratigraphic interval in the upper crust for Hole 504B and Hole 1256D highlight the differences in Sr isotope character at different stratigraphic levels in the crust. To account for the different MORB and seawater ^{87}Sr/^{86}Sr compositions for each hole, Sr isotopes are expressed as the fraction of seawater Sr, where $F_{Sr} = (\text{Rock}_{measured} - \text{Rock}_{MORB})/(\text{SW}_{Sr} - \text{Rock}_{MORB})$.

1998a, 1998b). The ^{87}Sr/^{86}Sr profile of Hole 504B displays significantly more elevated values in the volcanic sequence. The upper ∼300 m of the sheeted dikes in Hole 504B show a similar range of ^{87}Sr/^{86}Sr to Hole 1256D, but the lower sheeted dikes in Hole 504B have ^{87}Sr/^{86}Sr only slightly elevated above MORB values.

When plotted as cumulative frequencies to account for the differences in population size, there are striking differences in the Sr isotope measurements for each stratigraphic level in Hole 504B

and 1256D (Fig. 4). For example, at 90% of the total population in the volcanic sequence, the $^{87}Sr/^{86}Sr$ in Hole 504B is 0.7045 compared to only 0.7033 in Hole 1256D, that may reflect the variation in the eruption and alteration styles in the two volcanic sequences. In contrast, at 90% of the sheeted dike complexes, the $^{87}Sr/^{86}Sr$ in Hole 1256D is significantly higher (0.7046) than for Hole 504B (0.7038). However, Holes 504B and 1256D are more similar on a crustal scale where the normalised cumulative frequencies for the entire lava–dike $^{87}Sr/^{86}Sr$ datasets are considered (Fig. 4D). This may suggest that although each stratigraphic section shows variable degrees of fluid/rock exchange, this variation averages out on an upper crustal scale. However, because Sr-exchange in the dikes principally occurs at high temperatures directly at the ridge axis whereas low temperature hydrothermal exchange in the lavas can endure for millions of year, there may be significant variability in the elemental and isotopic exchange fluxes between the oceans and ocean crust depending on spreading rate and magmatic accretion styles. This is important when quantifying other geochemical exchanges with the oceans, such as Mg, K, Li, Tl and S, where fluid–rock exchange is strongly linked to temperature.

4.2. Subsurface structure of the hydrothermal system in Hole 1256D

4.2.1. Fluid channelling in the volcanic sequence

The $^{87}Sr/^{86}Sr$ profile through the volcanic sequence records minimal Sr isotope exchange during low temperature alteration, in agreement with the limited development of secondary alteration minerals (Alt et al., 2010). Zones of fractured basalts are associated with elevated $^{87}Sr/^{86}Sr$ in breccias (e.g., 770 mbsf) and alteration patches (e.g., 865 mbsf) that reflect the precipitation of hydrothermal minerals within these permeable zones. In addition to these intervals, there are two horizons within the volcanic sequence where the $^{87}Sr/^{86}Sr$ of the host basalts are considerably higher.

The uppermost horizon occurs within the Lava Pond and must reflect low temperature off-axis fluid circulation. At the top of the massive flow in Hole 1256C there is a ∼80 cm interval partially altered to clay minerals that represents the upper, flow deformed margin. This interval has higher $^{87}Sr/^{86}Sr$ (0.70430–0.70728) relative to the flow interior $^{87}Sr/^{86}Sr$ (0.70305, n = 25), and has high alkali concentrations (e.g., Rb = 2–12 ppm), indicating that the top of the ponded lava flow formed a preferential route for seawater-dominated hydrothermal fluid flow. High $^{87}Sr/^{86}Sr$ ratios (0.70601) are also recorded in the top of a <1 m thick sheet flow immediately beneath the massive ponded flow and indicates the preferential flow of fluids beneath the Lava Pond as well as above it.

The second horizon of high $^{87}Sr/^{86}Sr$ is the "Red Brick Horizon" at ∼648 mbsf (Wilson et al., 2003). This thin (41 cm) horizon is partially recrystallised to celadonite, beidellite, K-feldspar, iron oxyhydroxide, quartz and calcite (Alt et al., 2010), and lies immediately above a ∼25 m-thick pile of massive lava flows (Teagle et al., 2012b). $^{87}Sr/^{86}Sr$ of the RBH is up to 0.70427, in contrast to samples immediately above and below that have $^{87}Sr/^{86}Sr$ typical of the volcanic sequence (0.70321 and 0.70302). This interval is associated with elevated $\delta^{18}O$ values (8.6‰), low δ^7Li (−1.0 to −2.3‰), and high Li (16.1–21.4 ppm, Gao et al., 2012), Rb (11–32 ppm), and Ba (9–43 ppm) concentrations relative to the surrounding rocks. Water/rock (w/r) ratios calculated from oxygen isotopes are also higher for the RBH (w/r = 0.5) compared to most of the volcanic sequence (w/r = 0.1) (Gao et al., 2012). The high $^{87}Sr/^{86}Sr$ are similar to the hydrothermal end member (∼0.705) which, combined with increased concentrations of Si and Fe (Teagle et al., 2006) indicates alteration by a hydrothermal fluid rather than seawater. However, the secondary mineral assemblage indicates alteration at low temperatures (∼60 °C, Alt et al., 2010)

indicating substantial cooling of the hydrothermal fluid or mixing with seawater.

Based on wireline electrofacies classification the ∼800 m-thick volcanic sequence in Hole 1256D contains >100 lava flows, of which massive flows make up 14% and are distributed throughout (Tominaga et al., 2009). Generally massive flows are 3–10 m thick and do not show strong Sr isotope exchange. Major shifts towards seawater compositions in whole rock $^{87}Sr/^{86}Sr$ are restricted to the upper margins of the two thickest massive lava flow sequences, both more than 25 m thick. The establishment of sustained major fluid channels that alter the host rock basalts as well as brecciated material therefore requires more than a flow margin. This suggests that due to their great thickness these particular massive flow sequences formed relatively impermeable barriers to fluid flow and caused fluids to become channelled along their tops.

Heat flow models of ocean ridge flanks explain the isothermal conditions of the uppermost basement through the lateral movement of large volumes of hydrothermal fluids across the ridge flanks (Fisher and Becker, 1995). Although regional heat flow patterns can be explained by lateral flow in the upper few hundred metres of lavas, models cannot determine where and how many channels may be present within the crust. Our results from Site 1256 are the first to identify the location of discrete zones of lateral, low temperature fluid flow within the upper crust, their thickness, and the likely role of thick massive lava flows as a control for the loci for ridge flank fluid flow.

4.2.2. Fluid channelling in the Lava–Dike Transition

The Lava–Dike Transition marks the step increase in the temperature of hydrothermal alteration with the onset of sub-greenschist facies mineral formation. The $^{87}Sr/^{86}Sr$ of sheet flows within the LDT are indistinct from the overlying lavas, indicating only limited fluid–rock interaction. In contrast, the multiple brecciated and Mg-saponite silica-sulphide mineralised horizons within the LDT record high $^{87}Sr/^{86}Sr$ and extensive fluid–rock reaction that leached Sr from the rocks (Figs. 3 and 5). The breccias are generally associated with $^{87}Sr/^{86}Sr$ compositions that are higher than the predicted hydrothermal fluid composition (∼0.705) requiring the input of seawater strontium. The LDT is an interface between downwelling seawater and upwelling high temperature hydrothermal fluids, and the high $^{87}Sr/^{86}Sr$ in the brecciated horizons likely represents the mixing of little evolved seawater and cooled upwelling hydrothermal fluid too cold for copper mineralisation.

4.2.3. Fluid channelling along dike margins

The sheeted dike complex in ocean crust forms by repeated dike intrusions that are associated with rapid changes in local permeability, resulting in spatial and temporal relationships between dike intrusions and perturbations to hydrothermal systems (Delaney et al., 1998; Lowell and Germanovich, 1995; Wilcock, 1997).

In Hole 1256D, the $^{87}Sr/^{86}Sr$ data record the intimate link between dike intrusion and hydrothermal fluid flow throughout the sheeted dikes. In addition to the pervasive fluid flow throughout the dike complex that results in partial recrystallisation to greenschist facies assemblages, there is strong evidence for channelled fluid flow along dike margins relative to dike cores (Fig. 6). The channelling of hydrothermal fluids along dike margins and thin dikelets is recorded by high $^{87}Sr/^{86}Sr$ (median = 0.7043, n = 38) compared to the dike cores (median = 0.7035, n = 151) (Fig. 6). The occurrence of chilled, brecciated, and Cu-sulphide-mineralised contacts throughout the dike complex indicates intrusion into an active hydrothermal system.

Hydrothermal circulation within the sheeted dikes must include both recharge and discharge components. Most models of
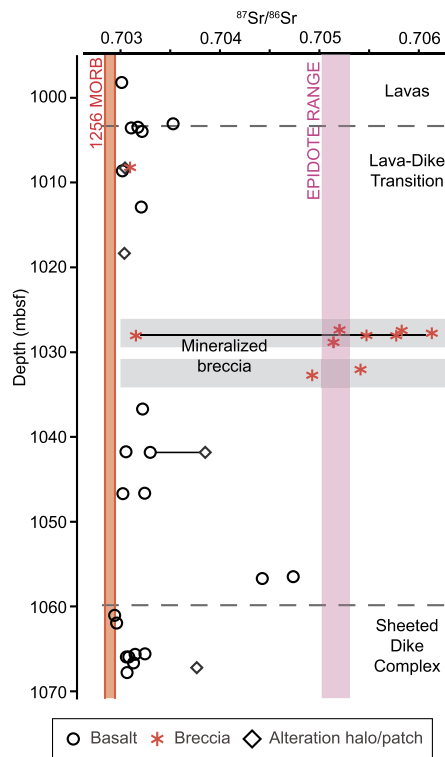
Fig. 5. Whole rock Sr isotope profile through the Lava–Dike Transition with discrete intervals of brecciation and silica-pyrite mineralisation accompanied by extensive fluid–rock reaction and Sr-isotope exchange. Breccia subsamples joined by tie lines.
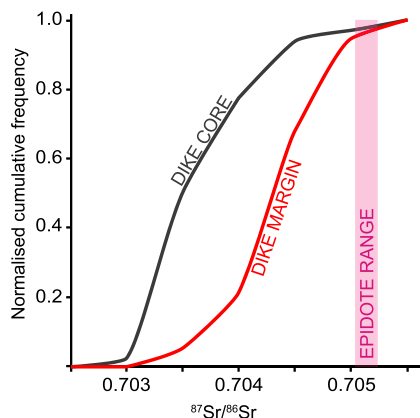

Fig. 6. Sr isotope evidence for channelled fluid flow along dike margins in the Sheeted Dike Complex. Normalised cumulative frequency for whole rock Sr isotopes from dike cores (n = 151) and dike margins (n = 38) shown relative to the predicted hydrothermal end member ^{87}Sr/^{86}Sr. Dike margins are associated with higher ^{87}Sr/^{86}Sr (median = 0.7043) relative to dike cores (median = 0.7035), reflecting more extensive fluid–rock interaction along dike margins indicating the preferential channelling of fluids along the margins.

MOR hydrothermal circulation postulate regional recharge with focused discharge, but there is as yet little information on the pathways by which seawater enters the intrusive layers of the ocean crust and subsequently expelled at vents (Coogan, 2008; Sleep, 1991). Evidence from ophiolites indicates that recharge through the dikes is pervasive (Bickle and Teagle, 1992) but maintaining greenschist facies metamorphic conditions in the sheeted dikes requires relatively low fluid fluxes (Teagle et al., 2003). Numerical simulations predict focused discharge in narrow (10–100s m wide) spatially transient upflow zones (Coumou et al., 2009). Secondary minerals along dike margins associated with high-temperature hydrothermal discharge fluids include chlorite ± epidote ± pyrite

± chalcopyrite ± quartz. Low-temperature minerals that may be associated with recharge fluids include anhydrite ± calcium carbonate ± chlorite-smectite ± K-feldspar (Hayman et al., 2009). The downhole distribution of these minerals along dike margins shows no trend with depth, with both recharge and discharge minerals present throughout, although the relative abundance of each mineral varies (Supplementary material D). All of the margins observed in the Hole 1256D cores contain both recharge and discharge secondary minerals, indicating that the dike margins provided pathways for both down and upwelling fluids. This is in accordance with recent microseismic observations of the EPR that indicate lateral migration of recharge and discharge zones at the ridge axis (Tolstoy et al., 2008). In ophiolites, focused upflow zones are associated with the formation of epidosites, equigranular epidote + quartz-rich rocks, that are present both along dike margins and within dike cores (Richardson et al., 1987; Schiffman et al., 1987). Epidosites are not observed in Hole 1256D, but some evidence for extensive hydrothermal alteration in dikes cores is documented by rare cm-scale alteration patches dominated by epidote + quartz assemblages with ^{87}Sr/^{86}Sr up to 0.70512.

Downhole wireline logging identified 86 subvertical, high-conductivity contacts in the Sheeted Dike Complex, and a further 28 isolated dikes within the volcanic sequence with the shallowest occurrence at ∼810 mbsf (Tominaga et al., 2009). Dike margins provide regularly spaced sub-vertical channels for recharge and discharge fluids and must be an important component in the structure of hydrothermal systems.

4.2.4. Fluid flow within the Dike–Gabbro Transition

The DGT marks the zone where fluid circulation in the upper crust is connected to the magma chamber heat source that drives the hydrothermal system. Previous studies have identified the Dike–Gabbro Transition as a temporally and spatially variable boundary, that can migrate vertically and horizontally in response to intrusions of sub-horizontal magma bodies, changes in the axial melt lens, and the hydrothermal system (Alt et al., 2010; Bergmanis et al., 2007; France et al., 2009; Gillis, 2008). The igneous and hydrothermal evolution of this zone recorded in Hole 1256D is complex and indicates a dynamic environment in which plutonic intrusion, contact metamorphism and hydrothermal circulation are intimately linked. The earliest stage of hydrothermal alteration of the lower sheeted dikes is overprinted by contact metamorphism (Alt et al., 2010). High seismic velocities measured by wireline geophysical tools confirm that the poorly recovered Granoblastic Dikes are continuous throughout this interval and indicate that the contact aureole (Teagle et al., 2006) is >150 m thick. Gabbro 1 and 2 have insufficient thermal mass to create this contact aureole (Coggon et al., 2008; Koepke et al., 2008). Together with granoblastic dike inclusions and unambiguous intrusive contacts, these bodies must represent relatively late-stage, yet on-axis, sub-horizontal intrusions of melt into the dikes that post date the contact metamorphism. Hydrothermal alteration after recrystallisation and intrusion is recorded by amphibole veins throughout the dike screens and plutonic rocks, further overprinted by lower temperature greenschist facies phases such as chlorite (Alt et al., 2010).

The elevated ^{87}Sr/^{86}Sr and high degrees of recrystallisation to secondary mineral assemblages at the upper boundaries for both Gabbro 1 and Gabbro 2 indicates that hydrothermal fluids were channelled along these boundaries (Fig. 7). The only limited increase in ^{87}Sr/^{86}Sr from MORB values and low vein abundances in the centres of the two gabbro bodies, indicate that fluid flow was not extensive through the cores of the gabbroic intrusions. The granoblastic dikes above and below the gabbro bodies may have contributed to this channelling by forming relatively impermeable barriers to fluid flow.
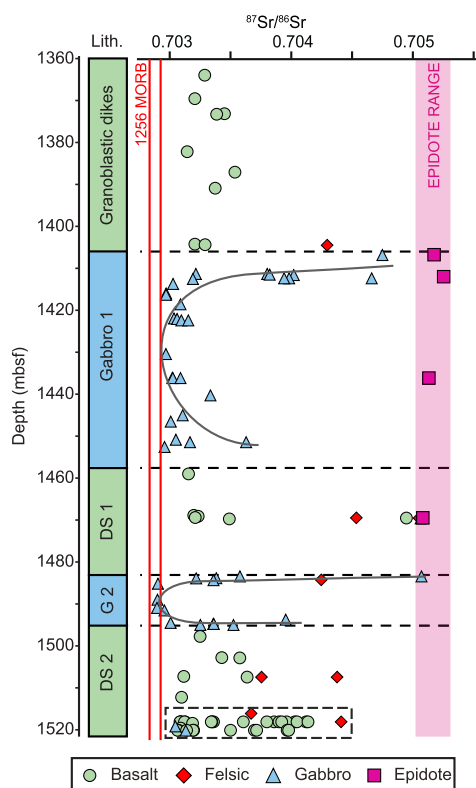
Fig. 7. Detailed lithostratigraphy with whole rock $^{87}Sr/^{86}Sr$ isotopes through the Dike–Gabbro Transition, shown relative to fresh Site 1256 MORB and the interpreted range for upwelling hydrothermal fluids from epidote mineral separates. Intrusive contacts between gabbro and granoblastic dikes are associated with $^{87}Sr/^{86}Sr$ elevated to hydrothermal fluid compositions, indicating that extensive fluid–rock reaction in the Dike–Gabbro Transition is restricted to intrusive margins, highlighted by the horseshoe shaped grey lines. Samples highlighted in the dashed box were recovered during remedial operations on Expedition 335 and are plotted at the maximum depth (Supplementary Material A).

The low value and limited range of $^{87}Sr/^{86}Sr$ in the Granoblastic Dikes (0.7032–0.7035), combined with recrystallised dike margins and dike cores having the same $^{87}Sr/^{86}Sr$, suggests that $^{87}Sr/^{86}Sr$ were homogenised during contact metamorphism. We interpret the decrease in $^{87}Sr/^{86}Sr$ through the base of the dike complex in Hole 1256D to be representative of the extent of hydrothermal exchange at the time when contact metamorphism occurred and not an artefact of low recovery in this section of the Hole. In contrast, Dike Screen 1 and 2 show a larger range in background $^{87}Sr/^{86}Sr$, and higher $^{87}Sr/^{86}Sr$ in alteration halos around veins and felsic intrusions that overprint the contact metamorphic recrystallisation, indicating later phases of hydrothermal reaction than recorded by the Granoblastic Dikes. This later hydrothermal alteration probably relates to fluid flow associated with the gabbro intrusions as the hydrothermal system extended into the DGT.

Seawater-like $^{87}Sr/^{86}Sr$ ratios (>0.706) have not been yielded by rocks or minerals from the intrusive sections of Hole 1256D. Nor have wireline image logs from Hole 1256D identified subvertical zones interpreted to be faults (Tominaga et al., 2009). This suggests that Hole 1256D has not intersected features that provided pathways for the direct ingress of seawater-like recharge fluids into the plutonic levels of the ocean crust, as are required by thermal models for the accretion of lower crust by sheeted sills (e.g., Maclennan et al., 2004).

4.3. Integrated crustal and hydrothermal evolution of Site 1256

The combination of the high resolution whole rock $^{87}Sr/^{86}Sr$ profile with detailed petrography, mineral geothermometry (this

study; Alt et al., 2010; Teagle et al., 2006, 2012a; Wilson et al., 2003) and wireline geophysical observations results in Hole 1256D (Tominaga et al., 2009; Tominaga and Umino, 2010) provides a unique opportunity to document the interconnections between crustal construction and hydrothermal circulation (Fig. 8). We present a four stage (T_1 to T_4) interpretation of the formation and evolution of the Site 1256 crust that is most consistent with the geochemical, petrographic and wireline observations, with relative time and distance based on a proposed sequence of volcanic eruption developed from Hole 1256D wireline measurements and observations from a modern mid-ocean ridge crest (Tominaga and Umino, 2010).

At T_1 the Site 1256 crust was located at the East Pacific Rise, and the stratigraphy includes the on-axis Sheet and Massive lava flows, a Lava–Dike Transition, and at least 400 m of Sheeted Dike Complex overlying some thickness of gabbro. Seawater penetrated into the crust, resulting in only minor alteration in the volcanic flows and consequently little modification of the downwelling fluid $^{87}Sr/^{86}Sr$. In the Lava–Dike Transition, seawater-like fluids mixed with upwelling hydrothermal fluids resulting in mineralisation of the breccia horizon at 130–180 °C (Alt et al., 2010). Some proportion of the downwelling seawater continued down into the Sheeted Dike Complex where water–rock reactions at greenschist facies temperatures resulted in the whole rock $^{87}Sr/^{86}Sr$ increasing from MORB values (~0.7029) to a mean of ~0.7033, with most of the hydrothermal exchange taking place in the upper portion of the dike complex. Fluids were channelled along dike margins, as evidenced by brecciated dikes and transects across dike margins that show higher $^{87}Sr/^{86}Sr$ than dike cores. In the lavas, horizontal flow boundaries provided fluid channels. Upwelling black smoker-type hydrothermal fluids are estimated to have $^{87}Sr/^{86}Sr$ of Hole 1256D epidote (070505–0.70525).

At T_2, Hole 1256D was still located at the ridge axis where the inflation of a magma lens resulted in the contact metamorphism of the lower 150 m of the Sheeted Dike Complex to granoblastic textures (~90 m of granoblastic dikes plus Dike Screen 1 and 2). The recrystallised basalts display a narrow range of elevated $^{87}Sr/^{86}Sr$ (0.7032–0.7034) that we attribute to isotopic homogenisation during contact metamorphism. This is evident from a contact metamorphosed dike margin, where no variation in $^{87}Sr/^{86}Sr$ is observed across the contact, in contrast to unrecrystallised dike margins where $^{87}Sr/^{86}Sr$ is significantly higher than dike cores. The mean of the recrystallised dikes is therefore interpreted to be representative of the mean $^{87}Sr/^{86}Sr$ in the lower dike complex prior to recrystallisation and intrusion of Gabbro 1 and 2. At this time the recrystallised Granoblastic Dikes acquired their final $^{87}Sr/^{86}Sr$ ratios because there is little petrographic evidence for post-recrystallisation hydrothermal alteration. Hydrothermal alteration in the upper Sheeted Dike Complex continues with both discharge and recharge fluids preferentially channelled along dike contacts, as evidenced by the secondary mineral assemblages and elevated $^{87}Sr/^{86}Sr$. The $^{87}Sr/^{86}Sr$ profile in the Sheeted Dike Complex approaches its final profile, with a large range in $^{87}Sr/^{86}Sr$ above the granoblastic dikes. Seawater continued to enter the crust and minor alteration of the most unstable phases (e.g., volcanic glass) in the volcanic sequence may have occurred (e.g., altered volcanic glass $^{87}Sr/^{86}Sr$ ~0.704). Mixing of seawater and hydrothermal fluids in the Lava–Dike Transition continued (Alt et al., 2010).

By T_3 the basement had moved off the axial rise and Site 1256 was sub-horizontal with the eruption of the first stage of off-axis volcanism (Inflated Flows). The intrusion of Gabbro 1 and 2, and the accompanying small felsic bodies into the recrystallised dikes had occurred. The igneous contacts of Gabbro 1 and 2 formed sub-horizontal channels for fluid flow resulting in higher $^{87}Sr/^{86}Sr$ and horseshoe-shaped isotope profiles. The felsic intrusions may include a component of partially melted hydrothermally altered
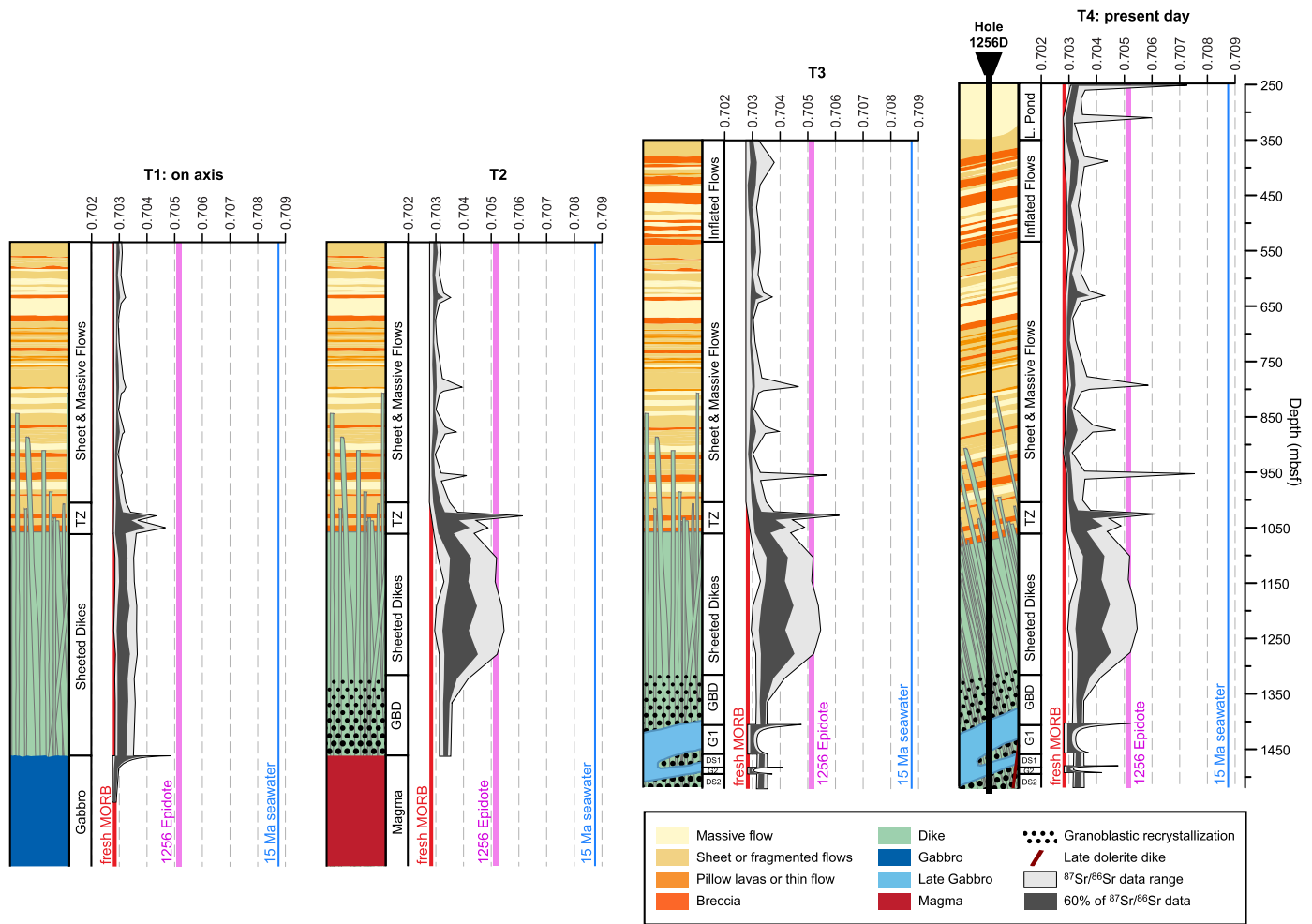
Fig. 8. Evolution of the Site 1256 Sr isotope profile through time. The evolution of Site 1256 is considered in four stages, T_1 to T_4, based on the progressive igneous construction of the crust (Tominaga and Umino, 2010) and petrographic observations of the evolving sequence of hydrothermal alteration. Constraints on the fluid composition through time and location in the crust arise from whole rock measurements and analyses of hydrothermal minerals separated from veins. GBD = Granoblastic Dikes, G1 = Gabbro 1. DS1 = Dike Screen 1, G2 = Gabbro 2, DS2 = Dike Screen 2.

rocks and therefore potentially a higher initial ^{87}Sr/^{86}Sr (Alt et al., 2010; France et al., 2009; Koepke et al., 2008). However, the high ^{87}Sr/^{86}Sr in both the adjacent host rock (gabbro or recrystallised dike) and the intrusions requires channelling of fluids through them after intrusion as the upper crustal hydrothermal system expanded down into the Dike–Gabbro Transition. Seawater continued to enter the upper crust and was likely channelled along flow boundaries and fractures.

T_4 represents the time from when Hole 1256D was >5 km from the ridge axis and the final stratigraphy was present with the Lava Pond emplaced onto crust rotated ~15° away from the ridge axis (Tominaga et al., 2009) to the present. In Dike Screen 2, a late dike was intruded and partially altered to greenschist facies minerals (^{87}Sr/^{86}Sr = 0.7035), suggesting some off-axis component of moderate temperature hydrothermal alteration in the DGT. Since T_4 Site 1256 experienced rapid sedimentation (>30 m/Myr) and together with the subdued regional basement topography due to the infill of the Lava Pond (Teagle et al., 2006), this may have protected much of the basement from extensive off-axis fluid flow. Within the lava sequence, prominent fluid channels were present and include the massive flow in the Lava Pond and the "Red Brick Horizon" where narrow regions of intense alteration are present above uncommonly thick (>25 m) sequences of massive flows.

5. Conclusions

- Hole 1256D has provided the opportunity to integrate the igneous construction of upper ocean crust with a temporally evolving hydrothermal system and the identification of fluid flow pathways in the crust.
- The whole rock Sr isotope profile through Hole 1256D shows limited increases in ^{87}Sr/^{86}Sr in the volcanic sequence, with evidence for channelled fluid flow at the top of thick (>25 m) massive flow sequences. There was only limited Sr isotope exchange between the lavas and low-temperature seawater-derived recharge fluids.
- The extent of hydrothermal alteration is less than observed in the pillow basalt-dominated volcanic sequence of Hole 504B. Hence, alteration of the upper crust is critically dependent on the style of volcanism and other factors such as basement relief, which may be a function of spreading rate.
- The Lava–Dike Transition is a mixing zone between downwelling recharge fluids and cooled upwelling high temperature discharge fluids, with fluid flow and most Sr-isotopic exchange occurring along discrete horizons of brecciation and silica-pyrite mineralisation.
- The Sheeted Dike Complex in Hole 1256D is dominated by pervasive increases in ^{87}Sr/^{86}Sr. However, dike margins have higher ^{87}Sr/^{86}Sr than dike cores and provided preferential

channels for recharge and discharge fluid flow in response to localised changes in permeability during dike intrusion.

- The first in situ recovery of the Dike–Gabbro Transition identifies this region to be dominated by channelled fluid flow along sub-horizontal igneous boundaries, with less Sr isotope exchange within the cores of the intruded gabbro bodies. Alteration halos around veins and thin felsic intrusions that postdate the contact metamorphism of the granoblastic dike screens within the DGT record the downward expansion of the upper crustal hydrothermal system.
- To date, only Holes 504B and 1256D have sampled sheeted dikes in intact ocean crust. The Sr isotopic profiles in these two holes are strikingly different, with a much greater extent of Sr-exchange in the sheeted dikes of the fast spread Site 1256 ocean crust. Although the overall extent of Sr-isotopic exchange in the whole upper crust (lavas and dikes) is similar in Holes 504B and 1256D, the highly elevated $^{87}Sr/^{86}Sr$ of dikes from Hole 1256D may have implications for the geochemical budgets of other elements mobilised by hydrothermal reactions at different temperatures (e.g., Li, Tl).

Acknowledgements

Appendix A. Supplementary material

Supplementary material related to this article can be found online at http://dx.doi.org/10.1016/j.epsl.2015.01.042.

References

Alt, J.C., 1995. Subseafloor processes in mid-ocean ridge hydrothermal systems. In: Humphris, S.E., Zierenberg, R.A., Mullineaux, L.S., Thomson, R.E. (Eds.), Seafloor Hydrothermal Systems: Physical, Chemical, Biological and Geological Interactions. In: Geophysical Monograph, vol. 91. AGU, Washington, pp. 85–114.

Alt, J.C., 2004. Alteration of the upper oceanic crust: mineralogy, chemistry, and processes. In: Davis, E.E., Elderfield, H. (Eds.), Hydrogeology of the Oceanic Lithosphere. Cambridge University Press, Cambridge, pp. 495–533.

Alt, J.C., Kinoshita, H., Stokking, L.B., et al., 1993. In: Proc. ODP Init. Repts., vol. 148. Ocean Drilling Program, College Station, TX.

Alt, J.C., Laverne, C., Coggon, R.M., Teagle, D.A.H., Banerjee, N.R., Morgan, S., Smith-Duque, C.E., Harris, M., Galli, L., 2010. Subsurface structure of a submarine hydrothermal system in ocean crust formed at the East Pacific Rise, ODP/IODP Site 1256. Geochem. Geophys. Geosyst. 11, Q10010.

Alt, J.C., Laverne, C., Vanko, D.A., Tartarotti, P., Teagle, D.A.H., Bach, W., Zuleger, E., Erzinger, E., Honnorez, J., Pezard, P., Becker, K., Salisbury, M.H., Wilkens, R.H., 1996a. Hydrothermal alteration of a section of upper oceanic crust in the eastern equatorial Pacific: a synthesis of results from Site 504 (DSDP Legs 69, 70 and 83, and ODP Legs 111, 137, 140 and 148). In: Proc. ODP Sci. Repts., vol. 148, pp. 417–434.

Alt, J.C., Teagle, D.A.H., 2000. Hydrothermal alteration and fluid fluxes in ophiolites and oceanic crust. Geological Society of America Special Paper 349, pp. 273–282.

Alt, J.C., Teagle, D.A.H., Laverne, C., Vanko, D.A., Bach, W., Honnorez, J., Becker, K., Ayadi, M., Pezard, P., 1996b. Ridge-flank alteration of upper ocean crust in the eastern Pacific: synthesis of results for volcanic rocks of Holes 504B and 896A. In: Proc. ODP Sci. Repts., vol. 148, pp. 435–450.

Bach, W., Humphris, S.E., 1999. Relationship between the Sr and O isotope compositions of hydrothermal fluids and the spreading and magma-supply rates at oceanic spreading centers. Geology 27, 1067–1070.

Bach, W., Peucker-Ehrenbrink, B., Hart, S.R., Blusztajn, J.S., 2003. Geochemistry of hydrothermally altered oceanic crust: DSDP/ODP Hole 504B – implications for seawater-crust exchange budgets and Sr- and Pb-isotopic evolution of the mantle. Geochem. Geophys. Geosyst. 4, 8904.

Bergmanis, E.C., Sinton, J., Rubin, K.H., 2007. Recent eruptive history and magma reservoir dynamics on the southern East Pacific Rise at 17°30′S. Geochem. Geophys. Geosyst. 8, Q12O06.

Bickle, M.J., Teagle, D.A.H., 1992. Strontium alteration in the Troodos ophiolite: implications for fluid fluxes and geochemical transport in mid-ocean ridge hydrothermal systems. Earth Planet. Sci. Lett. 113, 219–237.

Carbotte, S.M., Mutter, C., Mutter, J.C., Ponce-Correa, G., 1998. Influence of magma supply and spreading rate on crustal magma bodies and emplacement of the extrusive layer: insights from the East Pacific Rise at lat 16°N. Geology 26, 455–458.

Coggon, R.M., Alt, J.C., Teagle, D.A.H., 2008. Thermal history of ODP hole 1256D lower sheeted dikes: petrology, chemistry and geothermometry of the granoblastic dikes. Eos Trans. AGU 89 (53). Abstract V44B-06.

Coggon, R.M., Teagle, D.A.H., Smith-Duque, C.E., Alt, J.C., Cooper, M.J., 2010. Reconstructing past seawater Mg/Ca and Sr/Ca from mid-ocean ridge flank calcium carbonate veins. Science 327, 1114–1117.

Coogan, L.A., 2008. Reconciling temperatures of metamorphism, fluid fluxes, and heat transport in the upper crust at intermediate to fast spreading mid-ocean ridges. Geochem. Geophys. Geosyst. 9, Q02013.

Coogan, L.A., Dosso, S., 2012. An internally consistent, probabilistic, determination of ridge-axis hydrothermal fluxes from basalt-hosted systems. Earth Planet. Sci. Lett. 323, 92–101.

Coumou, D., Driesner, T., Geiger, S., Paluszny, A., Heinrich, C.A., 2009. High-resolution three-dimensional simulations of mid-ocean ridge hydrothermal systems. J. Geophys. Res. 114, B07104.

Delaney, J.R., Kelley, D.S., Lilley, M.D., Butterfield, D.A., Baross, J.A., Wilcock, W.S.D., Embley, R.E., Summit, M., 1998. The quantum event of oceanic crustal accretion: impacts of diking at mid-ocean ridges. Science 281, 222–230.

Fisher, A.T., Becker, K., 1995. Correlation between seafloor heat flow and basement relief: observational and numerical examples and implications for upper crustal permeability. J. Geophys. Res., Solid Earth 100, 12641–12657.

France, L., Ildefonse, B., Koepke, J., 2009. Interactions between magma and hydrothermal system in Oman ophiolite and in IODP Hole 1256D: fossilization of a dynamic melt lens at fast spreading ridges. Geochem. Geophys. Geosyst. 10, Q10O19.

Gao, Y., Vils, F., Cooper, K.M., Banerjee, N., Harris, M., Hoefs, J., Teagle, D.A.H., Casey, J.F., Elliott, T., Laverne, C., Alt, J.C., Muehlenbachs, K., 2012. Downhole variation of lithium and oxygen isotopic compositions of oceanic crust at East Pacific Rise, ODP Site 1256. Geochem. Geophys. Geosyst. 13, Q10001.

Gillis, K.M., 2008. The roof of an axial magma chamber: a hornfelsic heat exchanger. Geology 36, 299–302.

Hayman, N.W., Anma, R., Veloso, E.A., 2009. Data report: microstructure of chilled margins in the sheeted dike complex of IODP Hole 1256D. In: Teagle, D.A.H., Alt, J.C., Miyashita, S., Banerjee, N.R., Wilson, D.S. (Eds.), Proc. IODP, 309/312. IODP-MI Inc., Washington, DC.

Henstock, T.J., Woods, A.W., White, R.S., 1993. The accretion of oceanic-crust by episodic sill intrusion. J. Geophys. Res. 98, 4143–4161.

Höfig, T.W., Geldmacher, J., Hoernle, K., Hauff, F., Duggen, S., Garbe-Schönberg, D., 2014. From the lavas to the gabbros: 1.25 km of geochemical characterization of upper oceanic crust at ODP/IODP Site 1256, eastern equatorial Pacific. Lithos 210/211, 289–312.

Kelemen, P.B., Koga, K., Shimizu, N., 1997. Geochemistry of gabbro sills in the crust–mantle transition zone of the Oman ophiolite: implications for the origin of the oceanic lower crust. Earth Planet. Sci. Lett. 146, 475–488.

Kent, G.M., Harding, A.J., Orcutt, J.A., 1990. Evidence for a smaller magma chamber beneath the East Pacific Rise at 9°30′N. Nature 344, 650–653.

Koepke, J., Christie, D.M., Dziony, W., Holtz, F., Lattard, D., Maclennan, J., Park, S., Scheibner, B., Yamasaki, T., Yamazaki, S., 2008. Petrography of the dike–gabbro transition at IODP Site 1256 (equatorial Pacific): the evolution of the granoblastic dikes. Geochem. Geophys. Geosyst. 9, Q07O09.

Lowell, R.P., Germanovich, L.N., 1995. Dike injection and the formation of megaplumes at ocean ridges. Science 267, 1805–1807.

Maclennan, J., Hulme, T., Singh, S.C., 2004. Thermal models of oceanic crustal accretion: linking geophysical, geological and petrological observations. Geochem. Geophys. Geosyst. 5, Q02F25.

McArthur, J.M., Howarth, R.J., Bailey, T.R., 2001. Strontium isotope stratigraphy: LOWESS Version 3: best fit to the marine Sr-isotope curve for 0–509 Ma and accompanying look-up table for deriving numerical age. J. Geol. 109, 155–170.

Purdy, G.M., Kong, L.S.L., Christeson, G.L., Solomon, S.C., 1992. Relationship between spreading rate and the seismic structure of mid-ocean ridges. Nature 355, 815–817.

Richardson, C.J., Cann, J.R., Richards, H.G., Cowan, J.G., 1987. Metal-depleted root zones of the troodos ore-forming hydrothermal systems, Cyprus. Earth Planet. Sci. Lett. 84, 243–253.

Schiffman, P., Smith, B.M., Varga, R.G., Moores, E.M., 1987. Geometry, conditions and timing of off-axis hydrothermal metamorphism and ore-deposition in the Solea graben. Nature 325, 424–425.

Sleep, N.H., 1991. Hydrothermal circulation, anhydrite precipitation, and the thermal structure at ridge axes. J. Geophys. Res. 96, 2375–2387.

Teagle, D.A.H., Alt, J.C., Halliday, A.N., 1998a. Tracing the chemical evolution of fluids during hydrothermal recharge: constraints from anhydrite recovered in ODP Hole 504B. Earth Planet. Sci. Lett. 155, 167–182.

Teagle, D.A.H., Alt, J.C., Halliday, A.N., 1998b. Tracing the evolution of hydrothermal fluids in the upper oceanic crust: Sr-isotopic constraints from DSDP/ODP Holes 504B and 896A. Special Publications, vol. 148. Geological Society, London, pp. 81–97.

Teagle, D.A.H., Alt, J.C., Umino, S., Miyashita, S., Banerjee, N.R., Wilson, D.S., et al., 2006. Superfast spreading rate crust 2 and 3. In: Proc. IODP, 309/312. IODP-MI Inc., Washington, DC.

Teagle, D.A.H., Bickle, M.J., Alt, J.C., 2003. Recharge flux to ocean-ridge black smoker systems: a geochemical estimate from ODP Hole 504B. Earth Planet. Sci. Lett. 210, 81–89.

Teagle, D.A.H., Ildefonse, B., Blum, P., et al., 2012a. Superfast spreading rate crust 4. In: Proc. IODP, vol. 335. IODP-MI Inc., Tokyo.

Teagle, D.A.H., Smith-Duque, C.E., Harris, M., Rutter, J.E., Coggon, R.M., Tominaga, M., Alt, J.C., Murphy, B., Banerjee, N., 2012b. Anatomy of a deep sub-surface ridge flank aquifer: the "Red Brick" horizon in ODP Hole 1256D. In: Fall Meeting. AGU, California. Abstract OS13A-1693.

Tolstoy, M., Waldhauser, F., Bohnenstiehl, D.R., Weekly, R.T., Kim, W.-Y., 2008. Seismic identification of along-axis hydrothermal flow on the East Pacific Rise. Nature 451, 181–184.

Tominaga, M., Teagle, D.A.H., Alt, J.C., Umino, S., 2009. Determination of the volcanostratigraphy of oceanic crust formed at superfast spreading ridge: electrofacies analyses of ODP/IODP Hole 1256D. Geochem. Geophys. Geosyst. 10, Q01003.

Tominaga, M., Umino, S., 2010. Lava deposition history in ODP Hole 1256D: insights from log-based volcanostratigraphy. Geochem. Geophys. Geosyst. 11, Q05003.

Vance, D., Teagle, D.A.H., Foster, G.L., 2009. Variable quaternary chemical weathering fluxes and imbalances in marine geochemical budgets. Nature 458, 493–496.

Wilcock, W.S.D., 1997. A model for the formation of transient event plumes above mid-ocean ridge hydrothermal systems. J. Geophys. Res., Solid Earth 102, 12109–12121.

Wilson, D.S., 1996. Fastest known spreading on the Miocene Cocos–Pacific plate boundary. Geophys. Res. Lett. 23, 3003–3006.

Wilson, D.S., Teagle, D.A.H., Acton, G.D., et al., 2003. An in situ section of upper oceanic crust formed by superfast seafloor spreading. In: Proc. ODP Init. Repts., vol. 206. ODP, College Station, TX.

Wilson, D.S., Teagle, D.A.H., Alt, J.C., Banerjee, N.R., Umino, S., Miyashita, S., Acton, G.D., Anma, R., Barr, S.R., Belghoul, A., Carlut, J., Christie, D.M., Coggon, R.M., Cooper, K.M., Cordier, C., Crispini, L., Durand, S.R., Einaudi, F., Galli, L., Gao, Y., Geldmacher, J., Gilbert, L.A., Hayman, N.W., Herrero-Bervera, E., Hirano, N., Holter, S., Ingle, S., Jiang, S., Kalberkamp, U., Kerneklian, M., Koepke, J., Laverne, C., Vasquez, H.L.L., Maclennan, J., Morgan, S., Neo, N., Nichols, H.J., Park, S.-H., Reichow, M.K., Sakuyama, T., Sano, T., Sandwell, R., Scheibner, B., Smith-Duque, C.E., Swift, S.A., Tartarotti, P., Tikku, A.A., Tominaga, M., Veloso, E.A., Yamasaki, T., Yamazaki, S., Ziegler, C., 2006. Drilling to Gabbro in Intact Ocean Crust. Science 312, 1016–1020.